PHYSICAL REVIEW A VOLUME 47, NUMBER 6 JUNE 1993

Energy migration in molecular aggregates induced by stochastic coupling

A. S. Cordan, A. J. Boeglin, and A. A. Villaeys
Institut de Physique et Chimie des Materiaux de Strasbourg, Groupe d'Optique Nonlinéaire et d'Optoélectronique,
5 rue de l'Université, 67084 Strasbourg CEDEX, France

(Received 28 December 1992)

In the present paper, we report a theoretical description of the internal dynamics of one-dimensional molecular aggregates, subject to fluctuations of the excitation energy and site-site coupling. The role played by these diagonal and nondiagonal stochastic interactions on the nonlinear optical response of the aggregate is studied. As an example, the influence of these processes on the third-order hyperpolarizability is evaluated.

PACS number(s): 42.65.−k

I. INTRODUCTION

Over the last few years, considerable interest has been directed toward understanding the optical properties of molecular aggregates involved in media as different as molecular beams [1,2], solutions [3], or surfaces [4], and has spurred intense activity. Since the observation of a strong narrowing and redshift in the absorption spectrum of certain dye molecules [5], often termed the *J* band [6,7], we have a signature of the existence of small aggregates. This observation has been attributed to motional narrowing of the inhomogeneous broadening of an excitonlike state [8]. In fact, among all the theoretical descriptions, the one-dimensional Frenkel exciton model has provided the simplest description to the internal dynamics of molecular aggregates [9].

Some recent spectroscopic studies, performed with hole-burning and accumulated-photon-echo experiments [10], have shown evidence that in strongly coupled aggregates the electronic excitation is delocalized, while for weakly coupled aggregates there is no *J* band formation, but instead an excitation trapping and polaron formation. In optically thin samples, the excited-state dynamics of *J* aggregates having intermolecular dipole-dipole coupling and a varying inhomogeneous broadening have firmly established that the enhanced fluorescence rate results from microscopic superradiance and that the cooperativity is determined by a coherence length which can be equal to or smaller than the aggregate size depending on the amount of dephasing [11]. As the homogeneous or inhomogeneous broadening is increased, the coherence length decreases inducing in turn the disappearance of the superradiant decay.

Further studies have shown an enhanced radiative decay rate that depends on aggregate size [10,12]. This enhanced radiative rate may result from the $N^{1/2}$ scaling of the transition dipole moment, which in turn, generates an N scaling of the radiative decay rate with aggregate size N. In fact, it has been shown that pure dephasing competes with the radiative damping [13], and this competition depends on the relative value of the pure dephasing with respect to the enhanced radiative rate. For increasing values of the pure dephasing, the enhanced radiative rate decreases up to the value of the radiative rate of the monomer which is recovered for very large pure dephasings.

The investigation of third-order nonlinear optical hyperpolarizability in molecular aggregates and its scaling with aggregate size has been very active in recent years. Since the volume-squared scaling of the third-order hyperpolarizability for semiconductor microcrystallites or quantum dots predicted by Hanamura [14], many theoretical works concerning the electronic behavior of molecules in restricted geometries have been published.

The size dependence of the third-order hyperpolarizability in linear molecular aggregates incorporating the one- and two-exciton states has been considered by Ishahara and Cho [15], as well as by Spano and Mukamel [16,17]. In addition, by taking advantage of a model based on a coupled set of anharmonic oscillators, Spano and Mukamel were able to establish the influence on the nonlinear optical properties when the N-molecule system ranges from the small-aggregate limit with an N^2 scaling to the bulk-crystal limit giving an N scaling [17].

Other works have emphasized the exciton motion in molecular aggregates. Their main goal has been the study of the coherence loss inherent to the exciton migration. To this end, microscopic models, including a quantum-mechanical description of the interaction between Frenkel excitons and the phonons of the surrounding heat bath, are required [18,19]. Because these models are very difficult to solve, stochastic descriptions have been introduced where the influence of the phonons is accounted for by correlated Gaussian stochastic processes. As long as the stochastic variables describing the fluctuations of the local excitation energy are δ correlated, the model can be handled. As an example, this approach has enabled the study of the coupled coherent and incoherent motions of excitons [20]. The influence of the fluctuations of both excitation energy and transfer matrix element on the line shape of optical absorption has also been evaluated under the same assumption [21]. This study has enabled the evaluation of the contributions to the linewidth resulting from the local and nonlocal fluctuations. An exactly solvable model for coherent and incoherent motion of exciton in organic crystals has also been developed [22]; it gives explicit results for the mean-square excitonic displacement [23], as well as for the diffusion constant [24].

Besides the linear optical properties of stochastic molecular systems, other works have been developed concerning the nonlinear optical responses, such as the third-order hyperpolarizability. However, to our knowledge, only the cases of diagonal stochastic interactions [25,26] or of correlated diagonal stochastic interactions between near-neighboring sites [27] have been discussed. Finally, some recent improvements have been achieved which go beyond the white-noise treatment of the stochastic processes. Among them, we can mention the study of the optical line shapes of one-dimensional excitons under the influence of heat bath with colored noise [28]. It has clearly been established that upon increasing the rate of the excitation-energy fluctuations a transition from static to dynamic disorder is observed. Also, the corresponding optical absorption line shapes which are asymmetric for slow fluctuations become Lorentzian for fast fluctuations. With a different approach, Sato and Shibata [29–31] have developed a theory based on the time-convolution equation formalism. In their work, only the linear optical response of the material system has been considered. Assuming a medium subject to fluctuations generated by a Gaussian process, the cases of diagonal and nondiagonal randomness have been studied. In a first step, the problem has been handled perturbatively up to second order [29], while higher-order contributions have been accounted for by using the partial cumulant expansion to calculate absorption spectra and density of states [30,31]. It is worth mentioning that their approach is not restricted to the Markovian limit.

It is our intent to study the influence of both the fluctuations of the local excitation energies and the site-site interactions. Because of the difficulties inherent to the cumulant method when nondiagonal stochastic interactions are present, we will just be concerned in this work with the δ-correlated case. In Sec. II we introduce the description of the aggregates. It is done in the local basis set as well as in terms of the exciton basis set. Next, we describe the general dynamical evolution in Sec. III and discuss the influence of the stochasticity on the one- and two-exciton states. In Sec. IV we derive a formal expression of $\chi^{(3)}$, the third-order susceptibility, which is explicitly evaluated in Sec. V. Finally, in Sec. VI we present the results concerning the role of the diagonal and nondiagonal fluctuations on the third-order hyperpolarizabilities, and we summarize our findings in the last section.

II. DESCRIPTION OF THE AGGREGATES

In order to give a theoretical description of the role played by intersite stochastic coupling on the third-order hyperpolarizability, a basis for the representation of the aggregates must be chosen. The model consists of a set of noninteracting molecular aggregates, each of them having N identical molecules with two electronic configurations, an electronic energy gap $\hbar\Omega$, and parallel transition dipole moments. As long as the temperature is sufficiently low, phonon interactions will be neglected.

For the problem at hand, two types of representation are of interest. The first one consists of a set of localized states which are given by

$$\begin{aligned} |g\rangle &= \prod_{j=1}^{N} |g_j\rangle \;, \\ |n\rangle &= \prod_{j\neq n,\; j=1}^{N} |g_j\rangle |e_n\rangle \;, \\ |l,m\rangle &= \prod_{l\neq j\neq m,\; j=1}^{N} |g_j\rangle |e_l\rangle |e_m\rangle \;, \end{aligned} \tag{2.1}$$

where $|g_j\rangle$ and $|e_j\rangle$ are the ground and excited states of molecule j. Therefore we have one ground state, N singly excited states, and $N(N-1)/2$ doubly excited states since, for our model, two excitations cannot reside on the same site. Of course, higher excited states must be introduced in the study of hyperpolarizability of order higher than three. Also, we will assume periodic boundary conditions, say, $|p\rangle=|p+N\rangle$, and $|p,p+n\rangle=|p+n,p\rangle=|p+n,p+N\rangle$. If the intersite coupling $\hbar V$ is restricted to nearest-neighboring molecules, the corresponding Hamiltonian takes the simple form

$$H_0=\sum_{p=1}^{N} \hbar\Omega b_p^\dagger b_p + \sum_{p=1}^{N} \hbar V[b_p^\dagger b_{p+1}+b_{p+1}^\dagger b_p] \;, \tag{2.2}$$

or in terms of its spectral decomposition

$$\begin{aligned} H_0 = {} & \sum_{p=1}^{N} \hbar\Omega|p\rangle\langle p| + \sum_{p=1}^{N} \hbar V[|p\rangle\langle p+1| + |p+1\rangle\langle p|] + \sum_{p=1}^{N} \sum_{n=1}^{(N-1)/2} 2\hbar\Omega|p,p+n\rangle\langle p,p+n| \\ & + \sum_{p=1}^{N} \sum_{n=2}^{N-1} \hbar V[|p,p+n\rangle\langle p+1,p+n| + |p+1,p+n\rangle\langle p,p+n|] \;. \end{aligned} \tag{2.3}$$

Now, because of the coupling, it is convenient to introduce a delocalized basis set of states which diagonalizes H_0. In such a way, we may introduce the one- and two-exciton states, denoted $|A_k\rangle$ and $|B_{K,q}\rangle$, respectively, and defined by

$$\begin{aligned} H_0|A_k\rangle &= \hbar\omega_k|A_k\rangle \;, \\ H_0|B_{K,q}\rangle &= \hbar\Omega_{K,q}|B_{K,q}\rangle \;, \end{aligned} \tag{2.4}$$

where excitonic states and their corresponding energies are given by

$$|A_k\rangle=\frac{1}{\sqrt{N}}\sum_{p=1}^{N}e^{i2\pi kp/N}|p\rangle ,$$

$$\hbar\omega_k=\hbar\Omega+2\hbar V\cos\left\{\frac{2\pi k}{N}\right\}, \quad k=0,\ldots,N-1 ,$$

$$|B_{K,q}\rangle=\frac{2}{N}\sum_{p=1}^{N}\sum_{n=1}^{(N-1)/2}e^{i2\pi K(2p+n)/N}\sin\left\{\frac{(2q-1)\pi n}{N}\right\} \times|p,p+n\rangle , \tag{2.5}$$

$$\hbar\Omega_{K,q}=2\left[\hbar\Omega+2\hbar V\cos\left\{\frac{2\pi K}{N}\right\}\cos\left\{\frac{(2q-1)\pi}{N}\right\}\right],$$

$$K=0,\ldots,N-1,\; q=1,\ldots,\frac{N-1}{2} .$$

Here, for the sake of simplicity, N is taken to be odd. Notice that only linear molecular aggregates of arbitrary size and free ends admit fermionic eigenfunctions. Therefore the one- and two-exciton states $|A_k\rangle$ and $|B_{K,q}\rangle$, which are eigenfunctions of H_0, cannot be eigenfunctions of a fermion number operator [32]. However, in the infinite limit, the fermion character is recovered. This is because in this limit, the eigenenergies of the two-exciton states are the sum of two different one-exciton energies and their corresponding two-exciton eigenfunctions are Slater determinants built up from the same one-exciton eigenfunctions [33].

From these representations, the transition dipole matrix elements can be evaluated, depending on the problem at hand. The spectral decomposition of the aggregate-field interaction takes the form

$$H_{\mathrm{AF}}(t)=-\mathbf{d}\cdot\mathbf{E}(\mathbf{r},t)\left[\mu_0(|A_0\rangle\langle g|+|g\rangle\langle A_0|)+\sum_{q=1}^{(N-1)/2}\mu_{0;0,q}(|B_{0,q}\rangle\langle A_0|+|A_0\rangle\langle B_{0,q}|)\right.$$
$$\left.+\sum_{k=1}^{N-1}\sum_{q=1}^{(N-1)/2}\mu_{2K;K,q}(|B_{K,q}\rangle\langle A_{2K}|+|A_{2K}\rangle\langle B_{K,q}|)\right] . \tag{2.6}$$

In the previous expression, we have introduced the notations μ_{mon} for the matrix element of the monomer dipole moment, and

$$\mu_0=N^{1/2}\mu_{\mathrm{mon}} \tag{2.7}$$

because only the totally symmetric state $|A_0\rangle$ carries oscillator strength from the ground state, and

$$\mu_{k;K,q}=4\mu_{\mathrm{mon}}N^{-1/2}\sum_{n=1}^{(N-1)/2}\sin\left\{\frac{(2q-1)\pi n}{N}\right\} \times\cos\left\{\frac{2\pi Kn}{N}\right\}\delta_{k,2K} , \tag{2.8}$$

which gives the selection rules for optical excitation from the other states of the one-exciton band. Finally, **d** stands for the unit vector characterizing the orientation of the dipole moments μ_{mon}. The redistribution of the transition dipole moments in the delocalized basis set is schematically depicted in Fig. 1.

III. DYNAMICAL EVOLUTION

The dynamical evolution of a one-dimensional cyclic aggregate, consisting of N coupled two-level systems interacting with the applied electromagnetic fields, is conveniently described, in the rotating-wave approximation, by the superradiant master equation

$$\frac{d\rho(t)}{dt}=\sum_{n=1}^{N}i\Omega[\rho(t),b_n^\dagger b_n]+\sum_{m,n=1}^{N}{}' \, i\Omega_{mn}[\rho(t),b_m^\dagger b_n]$$
$$+\sum_{m,n=1}^{N}\gamma_{mn}\{b_m\rho(t)b_n^\dagger -\tfrac{1}{2}[b_m^\dagger b_n\rho(t)+\rho(t)b_m^\dagger b_n]\}$$
$$-\frac{i\boldsymbol{\mu}_{\mathrm{mon}}}{\hbar}\cdot\sum_{n=1}^{N}\mathbf{E}(\mathbf{r}_n,t)[\rho(t),b_n^\dagger+b_n] , \tag{3.1}$$

first established by Lehmberg [34], and later extensively studied by Gross and Haroche [35]. Here, $\rho(t)$ is the density matrix of the aggregate, and the prime on the summation means $m\neq n$. The applied electric fields $\mathbf{E}(\mathbf{r}_n,t)$ and the Pauli creation and annihilation operators $b_n^\dagger$ and b_n are defined at site $\mathbf{r}_n$. These operators obey the anticommutation rules

$$[b_m^\dagger,b_n]_+=\delta_{mn}+2b_m^\dagger b_n(1-\delta_{mn}) ,$$
$$[b_n^\dagger,b_m^\dagger]_+=(1-\delta_{mn})2b_n^\dagger b_m^\dagger . \tag{3.2}$$

Notice that if the excitations are limited to a single site,

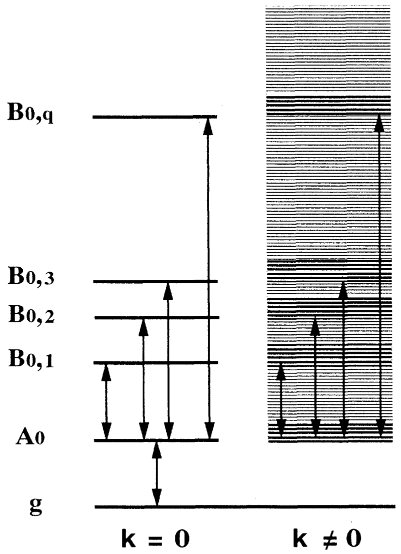

FIG. 1. Redistribution of the transition dipole moments in the one- and two-exciton basis set.

they behave like fermions, while for different sites they are bosons. Finally, $\boldsymbol{\mu}_{\text{mon}}$ is the monomer transition dipole moment, Ω the electronic energy gap, and the constants Ω_{mn} and γ_{mn} account for the excitation transfer and damping including spontaneous emission and superradiance. These quantities, respectively, reduce to V and γ in the long-wavelength limit and near-neighbor interactions. Notice that γ is the monomer spontaneous emission rate. Their explicit expressions have been established for the particular case of parallel dipole moments and can be found in the literature [11,35]. In addition, if we assume that the aggregate is small compared to an optical wavelength, its corresponding wave vector $\mathbf{k}$ satisfies the inequality $\mathbf{k}\cdot\mathbf{r}_{mn} \ll 1$, and consequently $\mathbf{E}(\mathbf{r}_n,t)$ will be approximated by $\mathbf{E}(\mathbf{r},t)$.

If we omit the interaction of the external fields with the aggregates, the evolution of the density matrix as given by Eq. (3.1) can be accounted for by the Liouvillian L_S defined by

$$
\begin{aligned}
L_S\rho(t) = {} & -\sum_{n=1}^{N} \hbar\Omega[\rho(t), b_n^\dagger b_n] - \sum_{m\neq n}^{N} \hbar V[\rho(t), b_m^\dagger b_n] \\
& + i \sum_{m,n=1}^{N} \hbar\gamma\{b_m\rho(t)b_n^\dagger \\
& \qquad - \tfrac{1}{2}[b_m^\dagger b_n\rho(t) + \rho(t)b_m^\dagger b_n]\} \ .
\end{aligned}
\tag{3.3}
$$

Besides the free evolution of the aggregates, we must introduce the description of the surrounding medium. Despite the fact that a stochastic description does not allow us to calculate the temperature dependence, it will be convenient for our purpose to construct a damping operator which accounts for the relaxation and dephasing processes induced by the surrounding medium. To this end, we introduce the stochastic part of the Liouvillian $\tilde{L}(t) = [\tilde{H}(t), \ ]$, where the Hamiltonian is defined by

$$
\begin{aligned}
\tilde{H}(t) = {} & \sum_{p=1}^{N} \varepsilon_p(t)|p\rangle\langle p| + \sum_{p=1}^{N} \vartheta_p(t)[|p\rangle\langle p+1| + |p+1\rangle\langle p|] + \sum_{p=1}^{N}\sum_{n=1}^{(N-1)/2} [\varepsilon_p(t) + \varepsilon_{p+n}(t)]|p,p+n\rangle\langle p,p+n| \\
& + \sum_{p=1}^{N}\sum_{n=2}^{N-1} \vartheta_p(t)[|p,p+n\rangle\langle p+1,p+n| + |p+1,p+n\rangle\langle p,p+n|] \ .
\end{aligned}
\tag{3.4}
$$

Here, the fluctuations are defined in the local basis. The quantity $\varepsilon_j(t)$ represents the fluctuations of the local excitation energy for the mono-excited and doubly excited states, while $\vartheta_j(t)$ describes the fluctuations of the intermolecular coupling between nearest-neighboring sites j and $j+1$, as depicted in Fig. 2. When the fluctuation time scale is very short with respect to all the other characteristic times of the aggregates, the correlation functions of the stochastic variables associated to the Gaussian Markov processes are δ correlated and satisfy the relations

$$
\begin{aligned}
&\langle \varepsilon_p(t) \rangle = 0 \ , \\
&\langle \varepsilon_p(t)\varepsilon_{p'}(t') \rangle = \hbar^2\gamma_0\delta_{pp'}\delta(t-t')
\end{aligned}
\tag{3.5}
$$

for the diagonal fluctuations, and

$$
\begin{aligned}
&\langle \vartheta_p(t) \rangle = 0 \ , \\
&\langle \vartheta_p(t)\vartheta_{p'}(t') \rangle = \hbar^2\gamma_1\delta_{pp'}\delta(t-t')
\end{aligned}
\tag{3.6}
$$

for the nondiagonal ones, where γ_0 and γ_1 stand for the fluctuation amplitudes. Because we are dealing with δ-correlated variables, the cumulant expansion method works and a stochastic damping operator can be defined [36]. Therefore the Liouville equation which governs the evolution is given by

$$
\frac{\partial\rho(t)}{\partial t} = -\frac{i}{\hbar}[L_S + \tilde{L}(t) + L_{\text{AF}}(t)]\rho(t) \ , \tag{3.7}
$$

if $L_{\text{AF}}(t) = [H_{\text{AF}}(t), \ ]$ stands for the interaction with the exciting fields. In the interaction representation, the formal zero-order solution with respect to $L_{\text{AF}}(t)$ corresponds to

$$
\rho_I^{(0)}(t) = \overleftarrow{\mathrm{T}} \exp\left\{ -\frac{i}{\hbar}\int_{t_i}^{t} dt_1 \tilde{L}_I(t_1) \right\} \rho_I(t_i) \ , \tag{3.8}
$$

where $\overleftarrow{\mathrm{T}}$ represents the chronological ordering operator and

$$
\begin{aligned}
&\rho_I(t) = e^{(i/\hbar)L_S t}\rho(t) \ , \\
&\tilde{L}_I(t) = e^{(i/\hbar)L_S t}\tilde{L}(t)e^{-(i/\hbar)L_S t} \ .
\end{aligned}
\tag{3.9}
$$

For Gaussian Markov processes with δ-correlated variables, the cumulant expansion reduces the expression of the averaged density matrix in the Schrödinger representation to the simple form

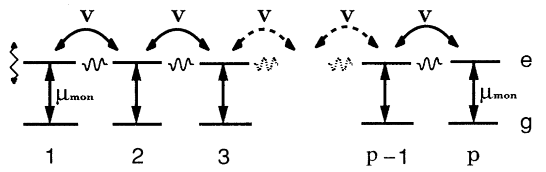

FIG. 2. Diagrammatic representation of the stochastic interactions acting on the aggregate. The broken line corresponds to the diagonal and the wavy lines to the nondiagonal stochastic couplings. Also shown are the coupling constant V and the dipole transition moments $\boldsymbol{\mu}_{\text{mon}}$.

$$\begin{aligned}\langle \rho^{(0)}(t)\rangle &= e^{-(i/\hbar)L_S t}\left\langle \overleftarrow{\mathrm{T}}\exp\left[-\frac{i}{\hbar}\int_{t_i}^{t}dt_1\tilde{L}_I(t_1)\right]\right\rangle e^{(i/\hbar)L_S t_i}\rho(t_i)\\ &= e^{-(i/\hbar)L_S t}\exp\left[-\frac{1}{\hbar^2}\int_{t_i}^{t}dt_1\int_{t_i}^{t_1}dt_2\langle \tilde{L}_I(t_1)\tilde{L}_I(t_2)\rangle\right]e^{(i/\hbar)L_S t_i}\rho(t_i)\ .\end{aligned} \tag{3.10}$$

From time derivation of $\langle \rho^{(0)}(t)\rangle$, the Liouville equation of the averaged density matrix

$$\frac{\partial\langle \rho^{(0)}(t)\rangle}{\partial t} = -\frac{i}{\hbar}[L_S - i\hbar\Gamma(t)]\langle \rho^{(0)}(t)\rangle \tag{3.11}$$

is straightforwardly established with

$$\Gamma(t) = \frac{1}{\hbar^2}\int_{t_i}^{t}dt'\langle \tilde{L}(t)e^{-(i/\hbar)L_S(t-t')}\tilde{L}(t')e^{(i/\hbar)L_S(t-t')}\rangle\ . \tag{3.12}$$

Consequently, in the Markovian limit, the stochastic damping operator Γ corresponding to the stochastic processes is given by

$$\Gamma = \frac{1}{\hbar^2}\int_{-\infty}^{\infty}dt'\langle \tilde{L}(t)e^{-(i/\hbar)L_S(t-t')}\tilde{L}(t')e^{(i/\hbar)L_S(t-t')}\rangle\ . \tag{3.13}$$

Because we assume the processes uncorrelated,

$$\Gamma = \Gamma_0 + \Gamma_1 \tag{3.14}$$

is the sum of two independent contributions, Γ_0 for the diagonal part and Γ_1 for the nondiagonal part. However, in both cases, their dynamical influence depends on the mixing induced by the averaged Liouvillian $\langle \tilde{L}(t)e^{-(i/\hbar)L_S(t-t')}\tilde{L}(t')e^{(i/\hbar)L_S(t-t')}\rangle$ on the excitonic states. As shown in the Appendix, we have no mixing in the $|A_k,g\rangle\rangle$ Liouvillian subspace, because the relations

$$\begin{aligned}&\Gamma_0|A_k,g\rangle\rangle = \gamma_0|A_k,g\rangle\rangle\ ,\\ &\Gamma_1|A_k,g\rangle\rangle = 2\gamma_1|A_k,g\rangle\rangle\end{aligned} \tag{3.15}$$

are satisfied. On the contrary, the diagonality is lost in the $|A_k,A_{k'}\rangle\rangle$ subspace, and the mixing results in the form

$$\begin{aligned}&\Gamma_0|A_k,A_{k'}\rangle\rangle = 2\gamma_0|A_k,A_{k'}\rangle\rangle - 2\frac{\gamma_0}{N}\sum_{k_1,k_2=0}^{N-1}\delta_{k_1-k_2,k-k'}|A_{k_1},A_{k_2}\rangle\rangle\ ,\\ &\Gamma_1|A_k,A_{k'}\rangle\rangle = 4\gamma_1|A_k,A_{k'}\rangle\rangle - 4\frac{\gamma_1}{N}\sum_{k_1,k_2=0}^{N-1}\delta_{k_1-k_2,k-k'}\left[\cos\left\{\frac{2\pi}{N}(k-k')\right\}+\cos\left\{\frac{2\pi}{N}(k+k_2)\right\}\right]|A_{k_1},A_{k_2}\rangle\rangle\ .\end{aligned} \tag{3.16}$$

Similarly, the mixing induced by Γ in the $|g,B_{K,q}\rangle\rangle$ subspace is described by the relations

$$\begin{aligned}\Gamma_0|g,B_{K,q}\rangle\rangle &= 2\gamma_0|g,B_{K,q}\rangle\rangle\ ,\\ \Gamma_1|g,B_{K,q}\rangle\rangle &= 4\gamma_1\left[1-\frac{2}{N}\sin^2\left\{\frac{(2q-1)\pi}{N}\right\}\right]|g,B_{K,q}\rangle\rangle\\ &\quad -8\frac{\gamma_1}{N}\sum_{q'\neq q,q'=1}^{(N-1)/2}\sin\left\{\frac{(2q-1)\pi}{N}\right\}\\ &\quad\times\sin\left\{\frac{(2q'-1)\pi}{N}\right\}\\ &\quad\times|g,B_{K,q'}\rangle\rangle\ .\end{aligned} \tag{3.17}$$

Finally, the action of Γ on the $|B_{K,q},A_k\rangle\rangle$ states has been developed in the Appendix and is given by

$$\begin{aligned}\Gamma_0|B_{K,q},A_k\rangle\rangle &= \sum_{K'=0}^{N-1}\sum_{q'=1}^{(N-1)/2}\sum_{k'=0}^{N-1}\Theta(K,q,k;K',q',k')\\ &\quad\times|B_{K',q'},A_{k'}\rangle\rangle\\ \Gamma_1|B_{K,q},A_k\rangle\rangle &= \sum_{K'=0}^{N-1}\sum_{q'=1}^{(N-1)/2}\sum_{k'=0}^{N-1}\Upsilon(K,q,k;K',q',k')\\ &\quad\times|B_{K',q'},A_{k'}\rangle\rangle\ ,\end{aligned} \tag{3.18}$$

where the functions $\Theta(K,q,k;K',q',k')$ and $\Upsilon(K,q,k;K',q',k')$ are given by relations (A3) and (A5).

From the previous expressions, it appears that after an optical excitation satisfying strict selection rules, the stochastic damping operator induces a redistribution of energy. Due to the nature of the coupling, we have no mixing between the subspaces corresponding to the Liouvillian states $|g,g\rangle\rangle$, $|A_k,g\rangle\rangle$, $|g,B_{K,q}\rangle\rangle$, and $|B_{K,q},A_k\rangle\rangle$. All these relations will be of interest, in the following, to evaluate the nonlinear optical properties of the molecular aggregate.

IV. INFLUENCE OF THE STOCHASTICITY ON THE NONLINEAR OPTICAL RESPONSE

As the dynamical evolution of the molecular aggregate interacting with its surrounding is known, the nonlinear response of the system to an optical excitation can be determined. We are interested here by the third-order hyperpolarizability which characterizes any four-wave-mixing process.

For a steady-state experiment, the electric fields have constant amplitudes E_j, and take the form

$$\mathbf{E}(\mathbf{r},t)=\sum_{j=a,b,c}[\boldsymbol{\epsilon}_j E_j e^{i(\mathbf{k}_j\cdot\mathbf{r}-\omega_j(t)}+\text{c.c.}] , \tag{4.1}$$

where c.c. denotes the complex-conjugate part, if ω_j, $\mathbf{k}_j$, and $\boldsymbol{\epsilon}_j$ are the frequency, wave vector, and unit polarization vector of the jth field, respectively. As usual, the third-order polarization is deduced from the third-order term of the time-dependent perturbation expansion of the density matrix. It can be expressed as

$$\mathbf{P}^{(3)}(\mathbf{r},t)=\text{Tr}[\langle\rho^{(3)}(\mathbf{r},t)\rangle\boldsymbol{\mu}] , \tag{4.2}$$

where the symbol Tr stands for the trace and the averaged density matrix of the molecular aggregate initially at equilibrium is given by

$$\langle\rho^{(3)}(\mathbf{r},t)\rangle=\frac{i}{\hbar^3}\int_{t_i}^{t}dt_3\int_{t_i}^{t_3}dt_2\int_{t_i}^{t_2}dt_1 G_0(t-t_3)L_{\text{AF}}(t_3)G_0(t_3-t_2)L_{\text{AF}}(t_2)G_0(t_2-t_1)L_{\text{AF}}(t_1)\rho(t_i) \tag{4.3}$$

because, in the Markovian limit, the factorization assumption is valid. Also, it is assumed that the aggregate is initially at equilibrium. Notice here that the Liouvillian $G_0(t-t')$ is defined by

$$G_0(t-t')=\Theta(t-t')e^{-(i/\hbar)[L_S-i\hbar\Gamma](t-t')} , \tag{4.4}$$

if $\Theta(t-t')$ stands for the Heaviside function. If the initial conditions are defined at $t_i=-\infty$, with a change of variables we get

$$\begin{aligned}\langle\rho^{(3)}(\mathbf{r},t)\rangle=-\frac{i}{\hbar^3}\sum_{p=a,b,c}\sum_{q=a,b,c,}\sum_{r=a,b,c}&(\mathbf{d}\cdot\boldsymbol{\epsilon}_p)(\mathbf{d}\cdot\boldsymbol{\epsilon}_q)(\mathbf{d}\cdot\boldsymbol{\epsilon}_r)\\ &\times\int_0^\infty dt_3\int_0^\infty dt_2\int_0^\infty dt_1 G_0(t_3)L_\mu G_0(t_2)L_\mu G_0(t_1)L_\mu\rho(t_i)\\ &\times\{E_p e^{i[\mathbf{k}_p\cdot\mathbf{r}-\omega_p(t-t_3)]}+\text{c.c.}\}\{E_q e^{i[\mathbf{k}_q\cdot\mathbf{r}-\omega_q(t-t_2-t_3)]}+\text{c.c.}\}\\ &\times\{E_r e^{i[\mathbf{k}_r\cdot\mathbf{r}-\omega_r(t-t_1-t_2-t_3)]}+\text{c.c.}\} ,\end{aligned} \tag{4.5}$$

where we have introduced the notation

$$L_{\text{AF}}(t)=-\mathbf{d}\cdot\mathbf{E}(\mathbf{r},t)L_\mu , \tag{4.6}$$

with $L_\mu=[\mu,]$. The formal development of the third-order polarization can be written in terms of its Fourier components as

$$\mathbf{P}^{(3)}(\mathbf{r},t)=\sum_\alpha[\mathbf{P}_\alpha^{(3)}(\omega_\alpha)e^{i(\mathbf{k}_\alpha\cdot\mathbf{r}-\omega_\alpha t)}+\text{c.c.}] , \tag{4.7}$$

where all the combinations

$$\begin{aligned}\mathbf{k}_\alpha&=\pm\mathbf{k}_p\pm\mathbf{k}_q\pm\mathbf{k}_r ,\\ \omega_\alpha&=\pm\omega_p\pm\omega_q\pm\omega_r ,\end{aligned} \tag{4.8}$$

are present and the indices p, q, and r run over a, b, and c. If we consider the particular combination $\mathbf{k}_\alpha=\mathbf{k}_a+\mathbf{k}_b+\mathbf{k}_c$ and $\omega_\alpha=\omega_a+\omega_b+\omega_c$, from the identification of Eqs. (4.2) and (4.7), we obtain

$$\begin{aligned}\mathbf{P}_\alpha^{(3)}(\omega_\alpha)=-\frac{i}{\hbar^3}\mathbf{d}\int_0^\infty dt_3\int_0^\infty dt_2\int_0^\infty dt_1 &\langle\langle\mu|G_0(t_3)L_\mu G_0(t_2)L_\mu G_0(t_1)L_\mu|g,g\rangle\rangle\\ &\times\sum_{\text{perm}}(\mathbf{d}\cdot\boldsymbol{\epsilon}_a)(\mathbf{d}\cdot\boldsymbol{\epsilon}_b)(\mathbf{d}\cdot\boldsymbol{\epsilon}_c)E_aE_bE_c e^{i(\omega_a+\omega_b+\omega_c)t_3}e^{i(\omega_a+\omega_b)t_2}e^{i\omega_a t_1}\end{aligned} \tag{4.9}$$

if the molecular aggregate is in its ground state at the initial time, so that $\rho(t_i)=|g,g\rangle\rangle$. Also, $\sum_{\text{perm}}$ stands for the 3! permutations over the fields since any ordering, involving the three different fields, participates only once.

At this stage, we can introduce the third-order hyperpolarizability from the formal expression

$$\mathbf{P}_\alpha^{(3)}(\omega_\alpha)=\chi^{(3)}(\omega_\alpha;\omega_a,\omega_b,\omega_c)\boldsymbol{\epsilon}_a E_a\boldsymbol{\epsilon}_b E_b\boldsymbol{\epsilon}_c E_c , \tag{4.10}$$

where

$$\chi^{(3)}(\omega_\alpha;\omega_a,\omega_b,\omega_c)=\sum_{\text{perm}} R^{(3)}(\omega_a+\omega_b+\omega_c,\omega_a+\omega_b,\omega_a)\mathbf{d}\otimes\mathbf{d}\otimes\mathbf{d}\otimes\mathbf{d} \tag{4.11}$$

and

$$R^{(3)}(\omega_a+\omega_b+\omega_c,\omega_a+\omega_b,\omega_a)=-\langle\langle\mu|G_0(\omega_a+\omega_b+\omega_c)L_\mu G_0(\omega_a+\omega_b)L_\mu G_0(\omega_a)L_\mu|g,g\rangle\rangle\ . \tag{4.12}$$

Notice that of the four **d**'s, three of them are to be applied separately on the unit vector ϵ_j of the three different exciting fields, and the remaining one defines the polarization component. Also, we have introduced the definition of the frequency-dependent Green function

$$G_0(\omega)=-\frac{i}{\hbar}\int_0^\infty dt\, e^{i\omega t}G_0(t)=\frac{1}{\hbar\omega-L_S+i\hbar\Gamma}\ . \tag{4.13}$$

To get an explicit evaluation of the third-order hyperpolarizability, we have to evaluate $R^{(3)}(\omega_a+\omega_b+\omega_c,\omega_a+\omega_b,\omega_a)$. This calculation can only be done if we know the various couplings induced, in the Liouvillian space, by Γ and L_S. Concerning Γ, the couplings have been calculated previously and are given by Eqs. (3.15)–(3.18).

We still require the couplings induced by L_S in the Liouvillian space. To this end, we introduce a partition of L_S given by

$$L_S=L_0+L_1+L_2\ , \tag{4.14}$$

where the various terms correspond to

$$\begin{aligned}
L_0\rho(t)&=-\sum_{n=1}^{N}\hbar\Omega[\rho(t)\,,b_n^\dagger b_n]-\sum_{m\neq n}^{N}\hbar V[\rho(t),b_m^\dagger b_n]\ ,\\
L_1\rho(t)&=-i\sum_{m,n=1}^{N}\tfrac{1}{2}\hbar\gamma[b_m^\dagger b_n\rho(t)+\rho(t)b_m^\dagger b_n]\ ,\\
L_2\rho(t)&=i\sum_{m,n=1}^{N}\hbar\gamma b_m\rho(t)b_n^\dagger\ .
\end{aligned} \tag{4.15}$$

The first term L_0 is purely diagonal, as it can be seen from the eigenvalue problem of H_0 described by Eq. (2.4). However, this is not the case of the two other terms. The mixing induced by L_1 can be described by the following relations:

$$\begin{aligned}
L_1|A_k,g\rangle\rangle&=-\frac{i\hbar}{2}\gamma(k)|A_k,g\rangle\rangle\ ,\\
L_1|A_k,A_{k'}\rangle\rangle&=-\frac{i\hbar}{2}[\gamma(k)+\gamma(k')]|A_k,A_{k'}\rangle\rangle\ ,\\
L_1|B_{K,q},g\rangle\rangle&=-i\hbar\xi(K,q)|B_{K,q},g\rangle\rangle\\
&\quad-i\hbar\sum_{q'=1,q'\neq q}^{(N-1)/2}\xi'(K,q,q')|B_{K,q'},g\rangle\rangle\ ,\\
L_1|B_{K,q},A_k\rangle\rangle&=-i\hbar[\xi(K,q)+\tfrac{1}{2}\gamma(k)]|B_{K,q},A_k\rangle\rangle\\
&\quad-i\hbar\sum_{q'=1,q'\neq q}^{(N-1)/2}\xi'(K,q,q')|B_{K,q'},A_k\rangle\rangle\ ,
\end{aligned} \tag{4.16}$$

where

$$\gamma(k)=N\gamma\delta_{k,0}\ , \tag{4.17}$$

and the functions $\xi(K,q)$ and $\xi'(K,q,q')$ are given by

$$\begin{aligned}
\xi(K,q)&=\frac{\gamma}{2N}\left\{\cot\left[\frac{(2q-1)+2K}{2N}\pi\right]\right.\\
&\qquad\left.+\cot\left[\frac{(2q-1)-2K}{2N}\pi\right]\right\}^2\ ,\\
\xi'(K,q,q')&=\frac{2\gamma}{N}\left\{\sum_{m,n=1}^{N-1}\sin\left[\frac{(2q-1)\pi m}{N}\right]\right.\\
&\qquad\times\sin\left[\frac{(2q'-1)\pi n}{N}\right]\\
&\qquad\left.\times\cos\left[\frac{2\pi K(m-n)}{N}\right]\right\}\ .
\end{aligned} \tag{4.18}$$

Finally, the last couplings of interest in the present model are induced by the Liouvillian L_2. They are described by the following relations:

$$\begin{aligned}
L_2|A_0,A_0\rangle\rangle&=i\hbar\gamma N|g,g\rangle\rangle\ ,\\
L_2|A_0,B_{0,q}\rangle\rangle&=2i\hbar\gamma\cot\left[\frac{(2q-1)\pi}{2N}\right]|g,A_0\rangle\rangle\ ,\\
L_2|B_{0,q},A_0\rangle\rangle&=2i\hbar\gamma\cot\left[\frac{(2q-1)\pi}{2N}\right]|A_0,g\rangle\rangle\ .
\end{aligned} \tag{4.19}$$

From the knowledge of these various couplings, the function $R^{(3)}(\omega_a+\omega_b+\omega_c,\omega_a+\omega_b,\omega_a)$ can be evaluated.

V. EVALUATION OF THE THIRD-ORDER HYPERPOLARIZABILITY

For the sake of convenience, we introduce in the explicit evaluation of the third-order hyperpolarizability some simplifying assumptions. While L_0 and L_2 will be treated exactly, we will neglect in the following some nondiagonal couplings introduced by L_1 and Γ. With respect to L_1, the range of validity of this assumption has been discussed previously [25] and is given by the condition $N^3\gamma \ll V\pi^2$. The second assumption is on the stochastic damping operator Γ. Here, we must distinguish two types of assumptions. The nondiagonal terms can be neglected in the subspace $|B_{K,q},g\rangle\rangle$, as long as the condition $N\gamma_1 \ll V\pi^2$ is satisfied. However, rejecting the nondiagonal terms in the subspace $|B_{K,q},A_k\rangle\rangle$ is more restrictive because, here, the condition $8N^2(\gamma_0+5\gamma_1)\ll V$ is required. Notice that all the previous conditions have been obtained by assuming that the various nondiagonal matrix elements are small compared to the corresponding energy levels.

The last difficulty, which needs to be overcome to evaluate the third-order hyperpolarizability, is the particular role played by that part of the stochastic operator corresponding to the nondiagonal stochastic interaction Γ_1. Its introduction in the complete dynamics of the aggregate is quite tedious. Because the ratio of γ_1 over γ_0 is generally small [22], a first-order perturbational treatment of Γ_1 on the subspace $|A_k, A_{k'}\rangle\rangle$ can be introduced. The iterative development of $G_0(\omega)$ given by

$$G_0(\omega)=\sum_{n=0}^{\infty} G_0^{(0)}(\omega)[-i\hbar\Gamma_1 G_0^{(0)}(\omega)]^n \tag{5.1}$$

is obtained from Eq. (4.13). Therefore, in this subspace, we get successively for the zero-order term

$$G_0^{(0)}(\omega)=\frac{1}{\hbar\omega-L_S+i\hbar\Gamma_0}\ , \tag{5.2}$$

the matrix element

$$\begin{aligned}\langle\langle A_k, A_k|G_0^{(0)}(\omega)|A_{k'}, A_{k'}\rangle\rangle=&\frac{1}{\hbar}\left[\frac{\delta_{k',0}}{\omega+iN\gamma+2i\gamma_0}+\frac{(1-\delta_{k',0})}{\omega+2i\gamma_0}\right]\\&\times\left\{\delta_{k,k'}+\frac{2i\gamma_0}{N}\frac{(\omega+2i\gamma_0)(\omega+2i\gamma_0+iN\gamma)}{(\omega+i\gamma_+)(\omega+i\gamma_-)}\left[\frac{\delta_{k,0}}{\omega+iN\gamma+2i\gamma_0}+\frac{(1-\delta_{k,0})}{\omega+2i\gamma_0}\right]\right\}\ ,\end{aligned} \tag{5.3}$$

where we have introduced the notation

$$\gamma_\pm=\tfrac{1}{2}[N\gamma+2\gamma_0]\pm\tfrac{1}{2}[(N\gamma+2\gamma_0)^2-8\gamma\gamma_0]^{1/2}\ . \tag{5.4}$$

For the first order-term, the expression is similarly deduced from the relation

$$\begin{aligned}\langle\langle A_k, A_k|G_0^{(1)}(\omega)|A_0, A_0\rangle\rangle=&-i\hbar\sum_{k_1,k_2}\langle\langle A_k, A_k|G_0^{(0)}(\omega)|A_{k_1}, A_{k_1}\rangle\rangle\\&\times\langle\langle A_{k_1}, A_{k_1}|\Gamma_1|A_{k_2}, A_{k_2}\rangle\rangle\langle\langle A_{k_2}, A_{k_2}|G_0^{(0)}(\omega)|A_0, A_0\rangle\rangle\ ,\end{aligned} \tag{5.5}$$

where we have used the property that Γ_1 and $G_0^{(0)}$ couple populations to populations and coherences to coherences only. The expressions of the matrix elements of interest in the other subspaces are easily obtained by using the assumptions previously discussed. For the states $|A_k,g\rangle\rangle$ we have

$$\langle\langle A_k,g|G_0(\omega)|A_k,g\rangle\rangle=\frac{1}{\hbar[\omega-\omega_k]+i\hbar[\frac{1}{2}\gamma(k)+\gamma_0+2\gamma_1]}\ . \tag{5.6}$$

In the $|B_{K,q},g\rangle\rangle$ subspace, we obtain similarly

$$\langle\langle B_{K,q},g|G_0(\omega)|B_{K,q},g\rangle\rangle=\frac{1}{\hbar[\omega-\Omega_{K,q}]+i\hbar[\Gamma_{K,q;g}+\xi(K,q)]}\ , \tag{5.7}$$

if we introduce the notation

$$\begin{aligned}\Gamma_{K,q;g}&=\langle\langle B_{K,q},g|\Gamma|B_{K,q},g\rangle\rangle\\&=2\left\{(\gamma_0+2\gamma_1)-\frac{4\gamma_1}{N}\sin^2\frac{(2q-1)\pi}{N}\right\}\ ,\end{aligned} \tag{5.8}$$

still valid for Γ_0 and Γ_1. Finally, the last type of terms corresponding to the states $|B_{K,q}, A_k\rangle\rangle$ are given by the expression

$$\langle\langle B_{K,q}, A_k|G_0(\omega)|B_{K,q}, A_k\rangle\rangle=\frac{1}{\hbar[\omega-\Omega_{K,q}+\omega_k]+i\hbar[\Gamma_{K,q;k}+\xi(K,q)+\frac{1}{2}\gamma(k)]}\ , \tag{5.9}$$

where the restriction of Γ to its diagonal part is described by the complementary notation

$$\begin{aligned}\Gamma_{K,q;k}=&\langle\langle B_{K,q}, A_k|\Gamma|B_{K,q}, A_k\rangle\rangle\\=&3(\gamma_0+2\gamma_1)-\frac{8\gamma_1}{N}\sin^2\left\{\frac{(2q-1)\pi}{N}\right\}-\frac{16\gamma_0}{N^2}\sum_{n=1}^{(N-1)/2}\sin^2\left\{\frac{(2q-1)n\pi}{N}\right\}\\&-16\frac{\gamma_1}{N^2}\left[\cos\left\{\frac{2\pi(K-k)}{N}\right\}+\cos\left\{\frac{2\pi(K+k)}{N}\right\}\right]\\&\times\sum_{n=1}^{(N-1)/2}\sin\left\{\frac{(2q-1)\pi n}{N}\right\}\left[\sin\left\{\frac{(2q-1)\pi(n+1)}{N}\right\}+\sin\left\{\frac{(2q-1)\pi(n-1)}{N}\right\}\right]\ .\end{aligned} \tag{5.10}$$

The last required terms correspond to the nondiagonal matrix elements included by L_2. Notice that the evaluation of $R^{(3)}(\omega_a+\omega_b+\omega_c,\omega_a+\omega_b,\omega_a)$ implies the difference of the following matrix elements:

$$\begin{aligned}\langle\langle g,g|G_0(\omega)|g,g\rangle\rangle &= \frac{1}{\omega}\ ,\\ \langle\langle g,g|G_0^{(0)}(\omega)|A_0,A_0\rangle\rangle &= \frac{1}{\omega}-\frac{(\omega+i\gamma_+)(\omega+i\gamma_-)-2\gamma\gamma_0(N-1)+2i\gamma_0(\omega+2i\gamma_0)}{(\omega+iN\gamma+2i\gamma_0)(\omega+i\gamma_+)(\omega+i\gamma_-)}\ .\end{aligned} \tag{5.11}$$

In fact, the divergence due to the term $1/\omega$ is just an artifact since it can be seen from the previous relation that this dependence cancels. We still require the matrix element

$$\langle\langle A_0,g|G_0(\omega)|B_{0,q},A_0\rangle\rangle = \frac{2i\gamma\cot\{(2q-1)\pi/2N\}}{\hbar[\omega-\omega_0+i\gamma_0+2i\gamma_1+(i/2)N\gamma][\omega-\Omega_{0,q}+\omega_0+i\Gamma_{0,q;0}+(i/2)N\gamma+i\xi(0,q)]}\ . \tag{5.12}$$

The same expression holds for $\langle\langle g,A_0|G_0(\omega)|A_0,B_{0,q}\rangle\rangle$ provided that ω_0 and $\Omega_{0,q}$ are replaced by $-\omega_0$ and $-\Omega_{0,q}$.

Of course, the complete expression of the third-order hyperpolarizability is quite cumbersome. Nevertheless, because it constitutes the starting point of the numerical simulations presented in the next section, we give its explicit form, that is to say

$$R^{(3)}(\omega_a+\omega_b+\omega_c,\omega_a+\omega_b,\omega_a)=R_1+R_2+R_3+R_4\ , \tag{5.13}$$

where the various terms take the form

$$\begin{aligned}R_1 = &-\frac{\mu_0^4}{\hbar^2}\left\{\frac{1}{\omega_a+\omega_0+(i/2)N\gamma+i\gamma_0+2i\gamma_1}+\frac{1}{\omega_a-\omega_0+(i/2)N\gamma+i\gamma_0+2i\gamma_1}\right\}\\ &\times\left\{\frac{1}{\omega_a+\omega_b+\omega_c-\omega_0+(i/2)N\gamma+i\gamma_0+2i\gamma_1}-\frac{1}{\omega_a+\omega_b+\omega_c+\omega_0+(i/2)N\gamma+i\gamma_0+2i\gamma_1}\right\}\\ &\times\left\{\langle\langle A_0,A_0|G_0^{(0)}(\omega_a+\omega_b)+G_0^{(1)}(\omega_a+\omega_b)|A_0,A_0\rangle\rangle\right.\\ &\qquad\left.+\frac{1}{\hbar}\frac{(\omega_a+\omega_b+i\gamma_+)(\omega_a+\omega_b+i\gamma_-)-2\gamma\gamma_0(N-1)+2i\gamma_0(\omega+2i\gamma_0)}{(\omega_a+\omega_b+2i\gamma_0+iN\gamma)(\omega_a+\omega_b+i\gamma_+)(\omega_a+\omega_b+i\gamma_-)}\right\}\ ,\end{aligned} \tag{5.14}$$

$$R_2=-\frac{\mu_0^2}{\hbar^3}\sum_{q=1}^{(N-1)/2}\mu_{0;0,q}^2$$

$$\times\Bigg\{\frac{1}{[\omega_a+\omega_b+\omega_c-\omega_0+(i/2)N\gamma+i\gamma_0+2i\gamma_1][\omega_a+\omega_b-\Omega_{0,q}+i\xi(0,q)+i\Gamma_{0,q;g}]}$$

$$\times\frac{1}{\omega_a-\omega_0+(i/2)N\gamma+i\gamma_0+2i\gamma_1}$$

$$-\frac{1}{[\omega_a+\omega_b+\omega_c+\omega_0+(i/2)N\gamma+i\gamma_0+2i\gamma_1][\omega_a+\omega_b+\Omega_{0,q}+i\xi(0,q)+i\Gamma_{0,q;g}]}$$

$$\times\frac{1}{\omega_a+\omega_0+(i/2)N\gamma+i\gamma_0+2i\gamma_1}$$

$$-\frac{1}{\omega_a+\omega_b+\omega_c-\Omega_{0,q}+\omega_0+(i/2)N\gamma+i\Gamma_{0,q;0}+i\xi(0,q)}$$

$$\times\Bigg[\hbar\langle\langle A_0,A_0|G_0^{(0)}(\omega_a+\omega_b)+G_0^{(1)}(\omega_a+\omega_b)|A_0,A_0\rangle\rangle$$

$$\times\left\{\frac{1}{\omega_a+\omega_0+(i/2)N\gamma+i\gamma_0+2i\gamma_1}+\frac{1}{\omega_a-\omega_0+(i/2)N\gamma+i\gamma_0+2i\gamma_1}\right\}$$

$$+\frac{1}{[\omega_a+\omega_b-\Omega_{0,q}+i\xi(0,q)+i\Gamma_{0,q;g}][\omega_a-\omega_0+(i/2)N\gamma+i\gamma_0+2i\gamma_1]}\Bigg]$$

$$+\frac{1}{\omega_a+\omega_b+\omega_c+\Omega_{0,q}-\omega_0+(i/2)N\gamma+i\Gamma_{0,q;0}+i\xi(0,q)}$$

$$\times\Bigg[\hbar\langle\langle A_0,A_0|G_0^{(0)}(\omega_a+\omega_b)+G_0^{(1)}(\omega_a+\omega_b)|A_0,A_0\rangle\rangle$$

$$\times\left[\frac{1}{\omega_a+\omega_0+(i/2)N\gamma+i\gamma_0+2i\gamma_1}+\frac{1}{\omega_a-\omega_0+(i/2)N\gamma+i\gamma_0+2i\gamma_1}\right]$$

$$+\frac{1}{[\omega_a+\omega_b+\Omega_{0,q}+i\xi(0,q)+i\Gamma_{0,q;g}][\omega_a+\omega_0+(i/2)N\gamma+i\gamma_0+2i\gamma_1]}\Bigg]\Bigg\}, \tag{5.15}$$

$$R_3=-\frac{\mu_0^2}{\hbar^2}\sum_{K=1}^{N-1}\sum_{q=1}^{(N-1)/2}\mu_{2K;K,q}^2\Bigg\{\frac{1}{\omega_a+\omega_b+\omega_c+\Omega_{K,q}-\omega_{2K}+i\xi(K,q)+i\Gamma_{K,q;2K}}$$

$$-\frac{1}{\omega_a+\omega_b+\omega_c-\Omega_{K,q}+\omega_{2K}+i\xi(K,q)+i\Gamma_{K,q;2K}}\Bigg\}$$

$$\times\langle\langle A_{2K},A_{2K}|G_0^{(0)}(\omega_a+\omega_b)+G_0^{(1)}(\omega_a+\omega_b)|A_0,A_0\rangle\rangle$$

$$\times\left\{\frac{1}{\omega_a+\omega_0+(i/2)N\gamma+i\gamma_0+2i\gamma_1}+\frac{1}{\omega_a-\omega_0+(i/2)N\gamma+i\gamma_0+2i\gamma_1}\right\}, \tag{5.16}$$

$$R_4=-\frac{\mu_0^3}{\hbar^3}\sum_{q=1}^{(N-1)/2}\mu_{0;0,q}$$

$$\times\Bigg\{-2i\gamma\cot\left[\frac{(2q-1)\pi}{2N}\right]\frac{1}{[\omega_a+\omega_b+\omega_c-\omega_0+(i/2)N\gamma+i\gamma_0+2i\gamma_1]}$$

$$\times\frac{1}{[\omega_a+\omega_b+\omega_c-\Omega_{0,q}+\omega_0+(i/2)N\gamma+i\xi(0,q)+i\Gamma_{0,q;0}]}$$

$$\times\Bigg[\hbar\langle\langle A_0,A_0|G_0^{(0)}(\omega_a+\omega_b)+G_0^{(1)}(\omega_a+\omega_b)|A_0,A_0\rangle\rangle$$

$$\times\left[\frac{1}{\omega_a+\omega_0+(i/2)N\gamma+i\gamma_0+2i\gamma_1}+\frac{1}{\omega_a-\omega_0+(i/2)N\gamma+i\gamma_0+2i\gamma_1}\right]$$

$$+\frac{1}{[\omega_a-\omega_0+(i/2)N\gamma+i\gamma_0+2i\gamma_1][\omega_a+\omega_b-\Omega_{0,q}+i\xi(0,q)+i\Gamma_{0,q;g}]}\Bigg]$$

$$+2i\gamma\cot\left[\frac{(2q-1)\pi}{2N}\right]\frac{1}{[\omega_a+\omega_b+\omega_c+\omega_0+(i/2)N\gamma+i\gamma_0+2i\gamma_1]}$$

$$\times\frac{1}{[\omega_a+\omega_b+\omega_c+\Omega_{0,q}-\omega_0+(i/2)N\gamma+i\xi(0,q)+i\Gamma_{0,q;0}]}$$

$$\times\Bigg[\hbar\langle\langle A_0,A_0|G_0^{(0)}(\omega_a+\omega_b)+G_0^{(1)}(\omega_a+\omega_b)|A_0,A_0\rangle\rangle$$

$$\times\left[\frac{1}{\omega_a+\omega_0+(i/2)N\gamma+i\gamma_0+2i\gamma_1}+\frac{1}{\omega_a-\omega_0+(i/2)N\gamma+i\gamma_0+2i\gamma_1}\right]$$

$$+\frac{1}{[\omega_a+\omega_0+(i/2)N\gamma+i\gamma_0+2i\gamma_1][\omega_a+\omega_b+\Omega_{0,q}+i\xi(0,q)+i\Gamma_{0,q;g}]}\Bigg]\Bigg\}. \tag{5.17}$$

At this point, we have the explicit expression of the third-order hyperpolarizability which is required for the numerical calculations.

VI. NUMERICAL CALCULATIONS AND DISCUSSION

In this section, we present and discuss the role of the diagonal and nondiagonal fluctuations on the third-order hyperpolarizabilities. We want to emphasize the role of the nondiagonal fluctuations γ_1 and compare their contribution to the one of the diagonal fluctuations γ_0.

We treat two cases: the resonant case through a degenerate forward four-wave-mixing experiment, and the nonresonant case through a phase-conjugate four-wave-mixing experiment. By "resonant" or "nonresonant" we mean that the frequencies of the electric fields are close to or far off the monoexcitonic resonance $\omega_0=\Omega+2V$.

The nonlinear susceptibility has been studied as a function of the parameters N, γ_0, and γ_1. However, their relative magnitudes are subject to restrictions because of the approximations $\gamma_1 < \gamma_0$ and more importantly $8N^2(\gamma_0+5\gamma_1) \leq V$, made in the evaluation of $\chi^{(3)}$.

In the following, we are not interested in the superradiant limit, largely discussed by Spano and Mukamel [25], and γ_0 is taken to be much larger than $N\gamma$, with γ being the monomer spontaneous emission rate. Of course, this also means that for fixed values of γ, γ_0, and γ_1, the approximations made put a limit on the aggregate size. Notice that as is the case of J aggregates, the nearest-neighbor coupling V is considered to be negative. For our numerical simulations, we have chosen $V=-600$ cm^{-1}, $\gamma=10^{-3}$ cm^{-1}, and the monomer electronic energy gap Ω equal to 16 000 cm^{-1}.

A. Resonant case

In a degenerate forward four-wave-mixing experiment, three nearly collinear laser beams with the same frequency ω, and wave vectors $\mathbf{k}_1$, $\mathbf{k}_2$, and $\mathbf{k}_3$, respectively, propagate in a nonlinear medium. A signal with frequency ω is generated in the direction $\mathbf{k}_1-\mathbf{k}_2+\mathbf{k}_3$. However, we are not concerned with the propagation of the fields through the medium, and focus instead on the response of an aggregate. $\chi^{(3)}$ can be written as

$$\chi^{(3)}(\omega;\omega,\omega,-\omega)=R^{(3)}(\omega,0,\omega)+R^{(3)}(\omega,0,-\omega)+R^{(3)}(\omega,2\omega,\omega)\ , \qquad (6.1)$$

where we have expressed the permutations over the fields of Sec. IV as a sum of three terms. The frequency ω is scanned over a frequency interval centered at $\omega_0=\Omega+2V$, to be close to the monoexcitonic resonance. In this case, $\chi^{(3)}$ can be accurately simplified by

$$\chi^{(3)}(\omega;\omega,\omega,-\omega)=R_1(\omega,0,\omega)+R_1(\omega,0,-\omega)\ , \qquad (6.2)$$

keeping only the two terms being triply resonant for $\omega=\omega_0$ as seen in Eq. (5.14).

In Fig. 3, we first represent $|\chi^{(3)}(\omega;\omega,\omega,-\omega)|$ for $N=5$, $\gamma_0=1$ cm^{-1}, and γ_1 varying from 0 to 0.3 cm^{-1}. The curves are normalized to a peak height of unity to compare the different linewidths. As expected, these widths are increasing with γ_1. The full width at half maximum (FWHM) can be easily derived from Eqs. (6.2) and (5.14), and varies linearly with $(\gamma_0+2\gamma_1)$. Therefore the amplitude of the nondiagonal fluctuations, although smaller than the amplitude of the diagonal ones, contributes twice as much to the overall linewidth.

Next, in Fig. 4, we compare the linewidths of the monomer and the aggregate. Notice that the monoexcitonic resonance of the chain is shifted by $2V$ with respect to the monomer, reflecting the intermolecular coupling V. Therefore the line shapes are plotted against the detuning $\Delta\omega=\omega-\Omega$ for the monomer, and $\Delta\omega=\omega-\omega_0$ for the aggregate. Here, we have set γ_0 equal to 0.5 cm^{-1} and γ_1 to 0.05 cm^{-1}. First of all, notice that the linewidths are independent of the aggregate size. Numerical calculations for $N=5,7,9$ show that the line shapes are indistinguishable. This result is characteristic of the nonsuperradiant behavior considered here, with the relevant parameter $(\gamma_0+2\gamma_1)$ much larger than $N\gamma$. The same observation remains true for $\gamma_1=0$, where we recover the result discussed by Spano and Mukamel [25] far off the superradiant limit.

The second feature is the difference between the monomer and the aggregate's linewidth. This difference stems from the parameter γ_1, increasing the width of the aggregate compared to the monomer's, the latter lacking for obvious reasons any nondiagonal fluctuations. Indeed, when γ_1 is set equal to zero, the aggregate's linewidth exactly coincides with the monomer's.

In order to further characterize the effect of γ_1 and N on the nonlinear response of the aggregate, we integrate $|\chi^{(3)}|^2$ over the frequency ω,

$$A(N,\gamma_0,\gamma_1)=\int_{-\infty}^{+\infty}|\chi^{(3)}(\omega;\omega,\omega,-\omega)|^2 d\omega\ , \qquad (6.3)$$

so as to recover a quantity proportional to the total inten-

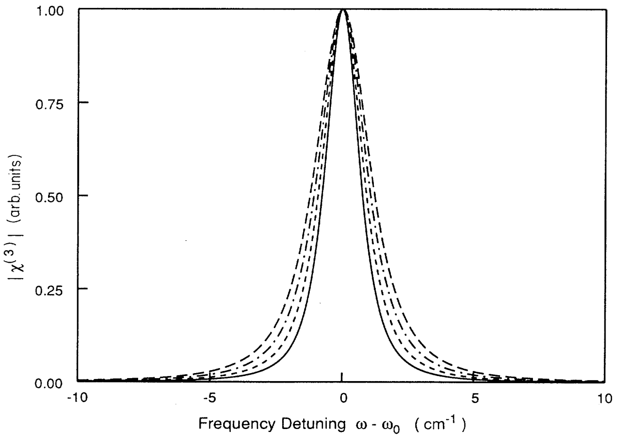

FIG. 3. Third-order hyperpolarizability $|\chi^{(3)}(\omega;\omega,\omega,-\omega)|$ vs detuning $(\omega-\omega_0)$ with $N=5$, $\gamma_0=1$ cm^{-1}, and $\gamma_1=0$, 0.1, 0.2, and 0.3 cm^{-1}. The curves are normalized to peak height of unity. Curves with increasing widths correspond to increasing values of γ_1.

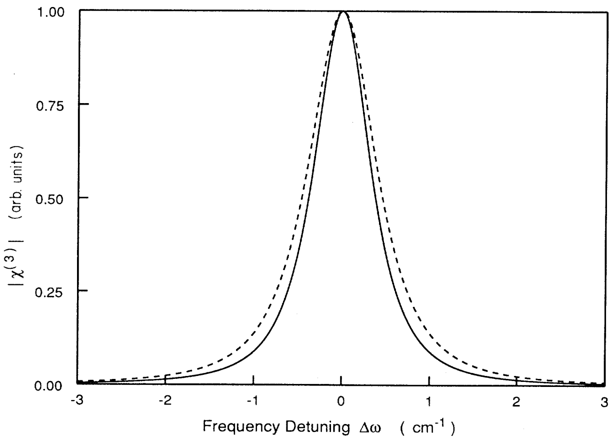

FIG. 4. Third-order hyperpolarizability $|\chi^{(3)}(\omega;\omega,\omega,-\omega)|$ vs detuning $\Delta\omega$ for the monomer and the aggregate, with $\gamma_0=0.5$ cm^{-1} and $\gamma_1=0.05$ cm^{-1}. The wider curve corresponds to the aggregate and the narrower one to the monomer. Only for $\gamma_1=0$ does the aggregate line shape coincide with the monomer's.

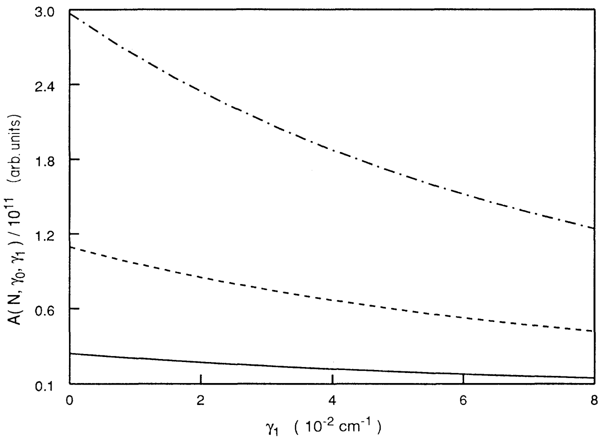

FIG. 5. $A(N,\gamma_0,\gamma_1)$ vs γ_1, close to resonance, with $\gamma_0=0.5$ cm^{-1}, and for several aggregate sizes $N=5,7,9$. A larger signal corresponds to a larger aggregate.

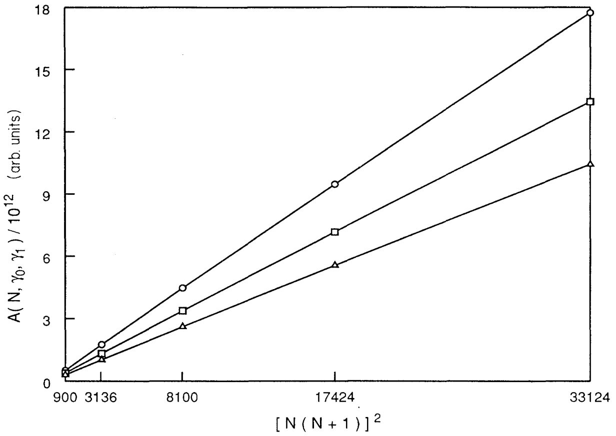

FIG. 6. $A(N,\gamma_0,\gamma_1)$ vs $[N(N+1)]^2$, close to resonance, with $\gamma_0=0.2$ cm^{-1} and for $\gamma_1=0$, 0.01, and 0.02 cm^{-1}. A lower signal corresponds to a larger value of γ_1.

sity of the recorded signal.

In Fig. 5, $A(N,\gamma_0,\gamma_1)$ is plotted versus γ_1, for several values of N, with γ_0 being held fixed at 0.5 cm^{-1}. As expected, close to resonance, $A(N,\gamma_0,\gamma_1)$ is a decreasing function of γ_1. In this case, it turns out that the total intensity of the signal times $(\gamma_0+2\gamma_1)^4$ behaves as a linear function of $(\gamma_0+2\gamma_1)$.

The dependence on N can be seen in Fig. 6, where the function $A(N,\gamma_0,\gamma_1)$ is depicted versus $[N(N+1)]^2$, for several values of γ_1, with γ_0 equal to 0.2 cm^{-1}. The straight lines observed show that near the resonance, $A(N,\gamma_0,\gamma_1)$ is proportional to $[N(N+1)]^2$, with the same type of enhancement over the monomer's response whether γ_1 is finite or whether it vanishes. This enhancement can be explained through the increased oscillator strength between the fundamental state $|g\rangle$ and the totally symmetric state $|A_0\rangle$. Again, as was shown in Fig. 5, $A(N,\gamma_0,\gamma_1)$ is a decreasing function of γ_1.

B. Nonresonant case

We now consider a phase-conjugate four-wave-mixing experiment with two pump beams and a probe beam propagating in a nonlinear medium. The wave vectors of the pumps are $\mathbf{k}_i$ and $\mathbf{k}_l$, with $\mathbf{k}_l=-\mathbf{k}_i$, and their frequency is ω_i. The wave vector and the frequency of the probe are $\mathbf{k}_j$ and ω_j, respectively. A phase-conjugate signal with frequency $2\omega_i-\omega_j$ is generated in the direction $\mathbf{k}_i-\mathbf{k}_j+\mathbf{k}_l=-\mathbf{k}_j$. Again notice that we are not concerned with the propagation of the fields through the medium.

This time, we write $\chi^{(3)}$ as

$$\chi^{(3)}(2\omega_i-\omega_j;\omega_i,-\omega_j,\omega i)=R^{(3)}(2\omega_i-\omega_j,\omega_i-\omega_j,\omega_i)+R^{(3)}(2\omega_i-\omega_j,\omega_i-\omega_j,-\omega_j)+R^{(3)}(2\omega_i-\omega_j,2\omega_i,\omega_i) . \tag{6.4}$$

The frequency ω_i is held fixed and ω_j is scanned over a narrow frequency interval centered at ω_i. In order to be far off resonance, we have chosen ω_i equal to ω_0+10V. It turns out that the linewidth of $|\chi^{(3)}|$ is the same whether γ_1 vanishes or not, because the FWHM is proportional to γ only, in the limit $\gamma_0 \gg N\gamma$ and far off resonance.

In Fig. 7, $A(N,\gamma_0,\gamma_1)$ is plotted versus γ_1, for several values of N, and $\gamma_0=0.5$ cm^{-1}. In this case, $A(N,\gamma_0,\gamma_1)$ is obtained by integrating $|\chi^{(3)}|^2$ over the frequency ω_j,

$$A(N,\gamma_0,\gamma_1)=\int_{-\infty}^{+\infty}|\chi^{(3)}(2\omega_i-\omega_j;\omega_i,-\omega_j,\omega i)|^2 d\omega_j . \tag{6.5}$$

In contrast to the resonant case, $A(N,\gamma_0,\gamma_1)$ is now an almost linearly increasing function of γ_1.

The dependence on N can be seen in Fig. 8, where $A(N,\gamma_0,\gamma_1)$ is depicted versus N^2, for several values of γ_1 and γ_0 fixed to 0.2 cm^{-1}. The straight lines scaled as

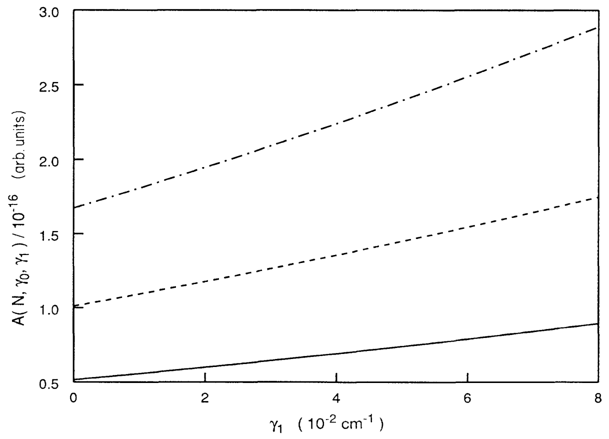

FIG. 7. $A(N,\gamma_0,\gamma_1)$ vs γ_1, far off resonance, with $\gamma_0=0.5$ cm^{-1}, and $N=5$, 7, and 9. A larger signal corresponds to a larger aggregate.

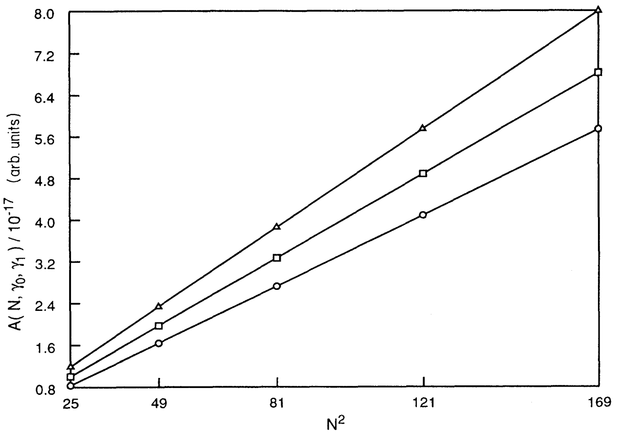

FIG. 8. $A(N,\gamma_0,\gamma_1)$ vs N^2, far off resonance, with $\gamma_0=0.2$ cm^{-1} and for $\gamma_1=0$, 0.01, and 0.02 cm^{-1}. A higher signal corresponds to a larger value of γ_1.

N^2 show that there is no enhancement with chain size, as was the case in the resonant process. As expected, for $\gamma_1=0$, one recovers N times the monomer result. Again, we observe that $A(N,\gamma_0,\gamma_1)$ is an increasing function of γ_1.

VII. CONCLUSION

In this work, we have studied the internal dynamics of small molecular aggregates ($\mathbf{k}\cdot\mathbf{r}_{mn} \ll 1$) subject to stochastic perturbations, and how they affect the nonlinear optical responses of the aggregates. This work, initially developed in the limit of diagonal stochastic perturbations, has been extended to include diagonal as well as nondiagonal couplings. Only the far-off-superradiant case has been considered here, with pure dephasing rates much larger than spontaneous emission rates.

For degenerate forward four-wave mixing, the total intensity of the signal displays an important enhancement with the aggregate size close to resonance. On the other hand, fluctuations in nondiagonal couplings efficiently reduce the integrated intensity.

The difference between the linewidths of an aggregate and a monomer stems from the nondiagonal parameter γ_1, pertaining to the chain only. The two widths coincide in absence of nondiagonal fluctuations.

For far-off-resonance phase-conjugate four-wave mixing, the total signal does not show any enhancement at all with size, but this time the intensity is an increasing function of γ_1. When γ_1 vanishes, one recovers N times the monomer result.

In this paper, we have shown that despite the fact that the nondiagonal amplitude γ_1 is smaller than the diagonal one γ_0, nondiagonal fluctuating couplings have a sizable effect on the nonlinear responses and optical line shapes.

So far, we have analyzed the contributions of independent diagonal and independent nondiagonal fluctuations to the nonlinear optical susceptibilities. In a forthcoming paper, we plan to compare the predictions of our model to those resulting from a model based on diagonal correlated stochastic fluctuations only.

Notice that only the Markovian limit has been considered here. It will be of interest, in the future, to describe the internal dynamics in the non-Markovian limit, for both diagonal and nondiagonal fluctuations, and to evaluate the resulting nonlinear responses of the aggregates in this case.

APPENDIX

As an example, we give here the evaluation of the mixing induced by the stochastic damping operator Γ. For the sake of simplicity, only the coupling generated by $\langle \tilde{L}(t_1)\tilde{L}(t_2)\rangle$ on the Liouvillian states $|B_{K,q},A_k\rangle\rangle = |B_{K,q}\rangle\langle A_k|$ is explicitly calculated. From the definition of the Liouvillian, we have

$$\langle \tilde{L}(t_1)\tilde{L}(t_2)\rangle |B_{K,q},A_k\rangle\rangle = |[\langle \tilde{H}(t_1)\tilde{H}(t_2)\rangle, |B_{K,q}\rangle\langle A_k|]_+\rangle\rangle - 2|\langle \tilde{H}(t_1)|B_{K,q}\rangle\langle A_k|\tilde{H}(t_2)\rangle\rangle\rangle \; . \tag{A1}$$

The evaluation of the first term $[\langle \tilde{H}(t_1)\tilde{H}(t_2)\rangle, |B_{K,q}\rangle\langle A_k|]_+$ can be obtained from the expression

$$\langle \tilde{H}(t_1)\tilde{H}(t_2)\rangle = \hbar^2\delta(t_1-t_2)\left\{\gamma_s \sum_{p=1}^{N} |p\rangle\langle p| + 2\gamma_s \sum_{p=1}^{N}\sum_{n=1}^{(N-1)/2} |p,p+n\rangle\langle p,p+n| - 2\gamma_1 \sum_{p=1}^{N} |p,p+1\rangle\langle p,p+1|\right\} , \tag{A2}$$

where the notation $\gamma_s=\gamma_0+2\gamma_1$ has been introduced. Using relation (2.5), we get the result

$$[\langle \tilde{H}(t_1)\tilde{H}(t_2)\rangle, |B_{K,q}\rangle\langle A_k|]_+ = \hbar^2\delta(t_1-t_2)\left\{3\gamma_s|B_{K,q}\rangle\langle A_k| - 4\frac{\gamma_1}{N^{3/2}}\sum_{p=1}^{N}\sum_{p'=1}^{N}\sin\left\{\frac{(2q-1)\pi}{N}\right\} e^{i2\pi K(2p+1)/N} \times e^{-i2\pi kp'/N}|p,p+1\rangle\langle p'|\right\} . \tag{A3}$$

Next, we must calculate the second term $\langle \tilde{H}(t_1)|B_{K,q}\rangle\langle A_k|\tilde{H}(t_2)\rangle$ of relation (A1). It can be obtained from the evaluation of the separate factors

$$\begin{aligned}\tilde{H}(t_1)|B_{K,q}\rangle=&\frac{2}{N}\sum_{p=1}^{N}\sum_{n=1}^{(N-1)/2}[\varepsilon_p(t_1)+\varepsilon_{p+n}(t_1)]\sin\left\{\frac{(2q-1)\pi n}{N}\right\}e^{i2\pi K(2p+n)/N}|p,p+n\rangle\\&+\frac{2}{N}\sum_{p=1}^{N}\sum_{n=1}^{(N-1)/2}\vartheta_p(t_1)\sin\left\{\frac{(2q-1)\pi n}{N}\right\}\\&\times[e^{i2\pi K(2p+2+n)/N}|p,p+n+1\rangle+(1-\delta_{1,n})e^{i2\pi K(2p+2-n)/N}|p,p+N+1-n\rangle\\&+e^{i2\pi K(2p-n)/N}|p+1,p+N-n\rangle+(1-\delta_{1,n})e^{i2\pi K(2p+n)/N}|p+1,p+n\rangle]\end{aligned}\tag{A4}$$

and

$$\tilde{H}(t_2)|A_k\rangle=\frac{1}{N^{1/2}}\sum_{p=1}^{N}\{\varepsilon_p(t_2)e^{i2\pi kp/N}|p\rangle+\vartheta_p(t_2)[e^{i2\pi k(p+1)/N}|p\rangle+e^{i2\pi kp/N}|p+1\rangle]\}\ .\tag{A5}$$

From these expressions, their product and statistical average must be performed. Therefore the mixing due to the diagonal fluctuations is given by the expressions

$$\Gamma_0|B_{K,q},A_k\rangle\rangle=\sum_{K'=0}^{N-1}\sum_{q'=1}^{(N-1)/2}\sum_{k'=0}^{N-1}\Theta(K,q,k;K',q',k')|B_{K',q'},A_{k'}\rangle\rangle\ ,\tag{A6}$$

where the function $\Theta(K,q,k;K',q',k')$ is defined by

$$\begin{aligned}&\Theta(K,q,k;K',q',k')\\&\quad=3\gamma_0\delta_{K,K'}\delta_{q,q'}\delta_{k,k'}-16\frac{\gamma_0}{N^2}\delta_{2(K-K'),k-k'}\sum_{n=1}^{(N-1)/2}\left[\sin\left\{\frac{(2q-1)\pi n}{N}\right\}\sin\left\{\frac{(2q'-1)\pi n}{N}\right\}\cos\left\{\frac{(K-K')2\pi n}{N}\right\}\right]\ .\end{aligned}\tag{A7}$$

Similarly, the mixing induced by the nondiagonal fluctuations corresponds to

$$\Gamma_1|B_{K,q},A_k\rangle\rangle=\sum_{K'=0}^{N-1}\sum_{q'=1}^{(N-1)/2}\sum_{k'=0}^{N-1}\Upsilon(K,q,k;K',q',k')|B_{K',q'},A_{k'}\rangle\rangle\ ,\tag{A8}$$

where the function $\Upsilon(K,q,k;K',q',k')$ is defined by

$$\begin{aligned}\Upsilon(K,q,k;K',q',k')=&6\gamma_1\delta_{K,K'}\delta_{q,q'}\delta_{k,k'}-8\frac{\gamma_1}{N}\sin\left[\frac{(2q-1)\pi}{N}\right]\sin\left[\frac{(2q'-1)\pi}{N}\right]\delta_{K,K'}\delta_{k,k'}\\&-16\frac{\gamma_1}{N^2}\delta_{2(K-K'),k-k'}\sum_{n=1}^{(N-1)/2}\Bigg\{\sin\left[\frac{(2q-1)\pi n}{N}\right]\sin\left[\frac{(2q'-1)\pi(n+1)}{N}\right]\\&\times\Bigg[\cos\left[\frac{2\pi}{N}[n(K-K')+(K'-k')]\right]\\&+\cos\left[\frac{2\pi}{N}[n(K-K')+(K'+k)]\right]\Bigg]\\&+\sin\left[\frac{(2q-1)\pi n}{N}\right]\sin\left[\frac{(2q'-1)\pi(n-1)}{N}\right]\\&\times\Bigg[\cos\left[\frac{2\pi}{N}[n(K-K')-(K'-k')]\right]\\&+\cos\left[\frac{2\pi}{N}[n(K-K')-(K'+k')]\right]\Bigg]\Bigg]\Bigg\}\ .\end{aligned}\tag{A9}$$

All the other types of mixing can be deduced similarly. Because their evaluations follow the same lines, they are not developed in this appendix.

[1] M. Y. Hahn and R. L. Whetten, Phys. Rev. Lett. **61**, 1190 (1988).
[2] U. Even, N. Ben-Horin, and J. Jortner, Phys. Rev. Lett. **62**, 140 (1989).
[3] K. Kemnitz, N. Tamai, I. Yamazaki, N. Nakashima, and K. Yoshihara, J. Phys. Chem. **90**, 5094 (1986).
[4] A. P. Alivisatos, M. F. Arndt, S. Efrima, D. H. Waldeck, and C. B. Harris, J. Chem. Phys. **86**, 6540 (1987).
[5] A. H. Hertz, Adv. Colloid Interface Sci. **8**, 237 (1977).
[6] G. Scheibe, Angew. Chem. **50**, 212 (1937).
[7] E. E. Jelly, Nature (London) **10**, 631 (1937).
[8] E. W. Knapp, Chem. Phys. **85**, 73 (1984).
[9] H. Fidder and D. A. Wiersma, Phys. Rev. Lett. **66**, 1501 (1991).
[10] S. De Boer, K. J. Vink, and D. A. Wiersma, Chem. Phys. Lett. **137**, 99 (1987).
[11] F. C. Spano and S. Mukamel, J. Chem. Phys. **91**, 683 (1989).
[12] V. Sundstrom, T. Gillbro, R. A. Gadonas, and A. Piskarskas, J. Chem. Phys. **89**, 2754 (1988).
[13] J. Grad, G. Hernandez, and S. Mukamel, Phys. Rev. A **37**, 3838 (1988).
[14] E. Hanamura, Phys. Rev. B **37**, 1273 (1988).
[15] H. Ishahara and K. Cho, Phys. Rev. B **42**, 1724 (1990).
[16] F. C. Spano and S. Mukamel, Phys. Rev. Lett. **66**, 1197 (1991).
[17] F. C. Spano and S. Mukamel, J. Chem. Phys. **95**, 7526 (1991).
[18] J. Köhler and P. Reineker, Chem. Phys. **93**, 209 (1985).
[19] R. G. Winkler and P. Reineker, Mol. Phys. **60**, 1283 (1987).
[20] H. Haken and G. Strobl, in *The Triplet State,* edited by A. B. Zahlan (Cambridge University Press, Cambridge, England, 1967).
[21] H. Haken and P. Reineker, Z. Phys. **249**, 253 (1972).
[22] H. Haken and G. Strobl, Z. Phys. **262**, 135 (1973).
[23] P. Reineker, Z. Phys. **261**, 187 (1973).
[24] P. Reineker and R. Kühne, Z. Phys. B **22**, 193 (1975).
[25] F. C. Spano and S. Mukamel, Phys. Rev. A **40**, 5783 (1989).
[26] J. A. Leegwater and S. Mukamel, Phys. Rev. A **46**, 452 (1992).
[27] O. Dubovsky and S. Mukamel, J. Chem. Phys. **95**, 7828 (1991).
[28] A. M. Jayannavar, B. Kaiser, and P. Reineker, Z. Phys. B **77**, 229 (1989).
[29] I. Sato and F. Shibata, Physica A **128**, 551 (1984).
[30] I. Sato and F. Shibata, Physica A **135**, 139 (1986).
[31] I. Sato and F. Shibata, Physica A **135**, 388 (1986).
[32] F. C. Spano, Phys. Rev. Lett. **67**, 3424 (1991).
[33] F. C. Spano, Chem. Phys. **96**, 8109 (1992).
[34] R. H. Lehmberg, Phys. Rev. **2**, 883 (1970).
[35] M. Gross and S. Haroche, Phys. Rep. **93**, 301 (1982).
[36] K. Faid and R. F. Fox, Phys. Rev. A **34**, 4286 (1986).